A Method for Reduction of Cogging Torque in Brushless DC Motor Considering the Distribution of Magnetization by 3DEMCN

Jin Hur and Dong-Seok Hyun
Dept. of Electrical Engineering, Hanyang University, Seoul 133-791, Korea

Jung-Pyo Hong
Dept. of Electrical Engineering, Changwon National University, Changwon 641-773, Korea

Abstract—**The method of reducing cogging torque and improving average torque has been studied by changing the dead zone angle of trapezoidal magnetization distribution of ring type rotor magnet in brushless DC motor(BLDCM). Because BLDCM has 3-D shape of overhang, 3-D analysis should be used for exact computation of its magnetic field. 3-D equivalent magnetic circuit network method(3-D EMCN) which can analyze an accurate 3-D magnetic field has been introduced. The analysis results of cogging torque using 3-D EMCN are compared with ones of 3-D finite element method(3-D FEM) and experimental data.**

Index terms-**Cogging torque, magnetization distribution, dead zone angle, overhang, 3-D EMCN, 3-D FEM.**

I. INTRODUCTION

Brushless permanent magnet DC motor(BLDCM) is widely used in industrial drives, computer peripheral devices and home automotive applications. It becomes smaller and higher power by use of high grade magnet. As a result, torque ripple is increased. Therefore, it is necessary to know accurately the flux distribution in the motor in order to decrease its torque ripple.

The torque ripple is mainly due to fluctuations of the field distribution and the armature MMF. Under dynamic conditions the torque ripple can be transmitted via the rotor to the coupled load, causing undesirable speed pulsations and inaccuracies in motion control at a low speed. Moreover through the stator frame, it induces vibrations, possible resonance, and acoustic noise. At high speeds, torque ripple is usually filtered out by the system inertia. The torque ripple contains both cogging torque and commutation torque components. Cogging torque which is due to the slotting on the stator or rotor is the primary ripple component in the torque generated in the BLDCM. It exists in all types of motor in which the airgap permeance is not constant.

Several methods have been used to reduce the cogging torque such as shoe of stator teeth, fractional pitch technique and skewing. Among the methods, the cogging torque can be reduced substantially by skewing either the stator teeth or the rotor magnet. However there are several disadvantages including the complexity of motor construction and the increase of leakage inductance [1], [2], [3].

Since, cogging torque is dependent on the pattern of magnetization distribution of magnet, it can also be minimized by changing the pattern [4], [5].

Manuscript received November 3, 1997.
J. Hur, +82-2-290-0349, fax +82-2-295-7111 hjin@hymail.hanyang.ac.kr,
D. S. Hyun, +82-2-290-0341, emcn@unitel.co.kr
J. P. Hong, +82-551-79-7517, tkso@chollian.dacom.co.kr,

If the effect of change pattern of magnetization distribution on torque ripple can be calculated, the reduction of torque ripple can be investigated without repeating a trial design.

The object of this paper is to suggest a method for the reduction of cogging torque and the improvement of average torque by choosing the reasonable value of dead zone angle from the magnetization distribution. The magnetization pattern of plastic *Nd-Fe-B* magnet in ring type is assumed to be trapezoidal. The dead zone is a weakly magnetized section of trapezoidal pattern and the variation of the dead zone angle has an effect on cogging torque as well as average torque. An increase of the dead zone angle to any extent effectively reduces cogging torque and improves average torque.

In this paper, in order to calculate cogging torque considering rotation of rotor magnet and overhang of which length is longer than the stator height in z direction, 3-D EMCN which can analyze 3-D magnetic field is introduced.3-D EMCN supplements magnetic equivalent circuit by numerical technique using distributive magnetic circuit parameter, permeance [6].

Then, the validity of suggested method is verified by comparing the simulation results with the 3-D finite element method(3-D FEM) and experimental one.

II. METHOD OF ANALYSIS

A.3-D EMCN and Analysis Model

Fig. 1. shows the cross section of analysis model. The exterior-rotor type BLDCM with 8 poles and 12 teeth is used for the analysis. The permanent magnets, ring type plastic Nd-Fe-B, are radially magnetized.

3-D EMCN is a numerical analysis technique that can support dynamic simulations taking the rotation of the armature into account.

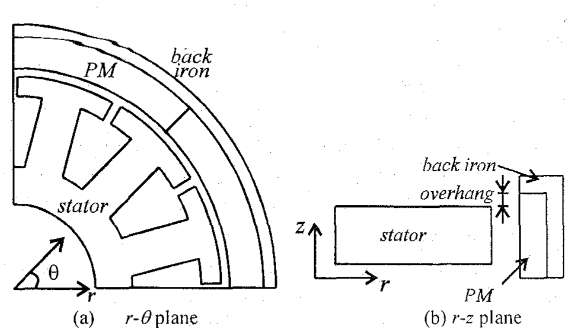

Fig.1. Analysis model.

0018-9464/98$10.00 © 1998 IEEE

3-D EMCN also, allows modeling of a machine in detail so that the discrete distribution of windings, stator and rotor slotting, and iron saturation can be included. This method divides the analysis model into elemental volumes (elements) of hexahedral shape according to regions, and then 3-D equivalent magnetic circuit network is constructed by connecting the centroids(nodes) of adjacent elements with adjacent element's permeance.

The fundamental r-directional node equation in (i,j,k) of the 3-D EMCN using scalar potential can be described by [6]:

$$\Phi_{r_{i,j-1,k}} = P_{r_{i,j-1,k}}\left(U_{i,j,k} - U_{i,j-1,k} + E_{i,j,k}\right) \qquad (1)$$

$$B_{r_{i,j-1,k}} = \Phi_{r_{i,j-1,k}} / S_{r_{i,j,k}} \qquad (2)$$

$$E_{i,j,k} = NI/m \qquad \text{at teeth region} \qquad (3)$$

$$= \frac{M\{\theta(i,j,k)\}}{\mu_0 \mu_r} r_{i,j,k} \qquad \text{at magnet region} \qquad (4)$$

where $\Phi r_{i,j-1,k}$ is magnetic flux, $Pr_{i,j-1,k}$ is permeance, $Br_{i,j-1,k}$ is magnetic flux density, $E_{i,j,k}$ is magnetomotive force of permanent magnet and stator current and $r_{i,j,k}$ is the magnetization depth of permanent magnet between nodes (i,j,k) and $(i,j\text{-}1,k)$. $U_{i,j,k}$ is unknown MSP and $M\{\theta(i,j,k)\}$ is magnetization of permanent magnet at node (i,j,k). N is the number of turns and m is the number of element of the teeth region in the r direction.

Magnetic flux continuity condition is applied at node (i,j,k) as following :

$$\Phi_{\theta_{i-1,j,k}} + \Phi_{\theta_{i+1,j,k}} + \Phi_{r_{i,j-1,k}} + \Phi_{r_{i,j+1,k}} + \Phi_{z_{i,j,k-1}} + \Phi_{z_{i,j,k+1}} = 0 \qquad (5)$$

From the magnetic flux of (1) and magnetic flux continuity condition that the sum of inflow and outflow of flux at node (i,j,k) is invariant as (5), the system matrix is constructed. The system matrix equation is given by

$$[\mathbf{P}]\{\mathbf{U}\} = \{\mathbf{F}\} \qquad (6)$$

where $[\mathbf{P}]$, permeance coefficient matrix is symmetric and produces good bandwidth and matrix sparsity patterns, $\{\mathbf{U}\}$ is matrix of node MSP, $\{\mathbf{F}\}$ is forcing matrix (=Permeance × MMF of stator current or PM). Magnetic flux density in machine is obtained from $\{\mathbf{U}\}$ calculated by using (1) and (2).

Torque is calculated by Maxwell Stress Tensor as the following.

$$\vec{T} = \int_S \left\{ \mu_0 \left(\vec{H}\cdot\vec{n}\right)\cdot\left(\vec{r}\times\vec{H}\right) - \frac{\mu_0}{2}\vec{H}^2\cdot\left(\vec{r}\times\vec{n}\right)\right\} d\vec{S} \qquad (7)$$

where $\vec{n}$, $\vec{r}$, and $\vec{H}$ are the normal vector to the surface S, the distance of a point to the axis of rotation, and the magnetic field.

III. Results and Discussion

A. Numerical and Experimental Verification

The magnetization pattern of permanent magnet is given in Fig. 2. A suitable model for the magnetization of the permanent magnet has to be chosen to determine coefficients of the Fourier series which is dependent on the cogging torque.

In 3-D EMCN it substitutes the movement of rotor for the movement of magnetization distribution in permanent magnet expressed by Fourier series so that it considers the movement of rotor simply by variation of magnetization distribution of forcing terms in system equation. Periodic conditions for the analysis model is also valid continuously without changing of it. Thus, it doesn't have to remesh the element due to the use of initial mesh continuously.

Fig. 3 shows radial and tangential magnetic flux density distribution according to the variation of dead zone angle θ_d in the air gap for aligned detent position. In radial magnetic flux density distribution, there is a distortion due to the tooth slotting structure of stator and leakage magnetic flux component. 3-D FEM is used to verify the analysis results by 3-D EMCN.

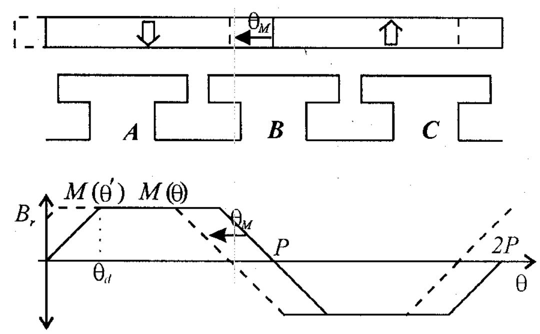

Fig. 2. Variation of magnetization distribution in permanent magnet with rotation angle.

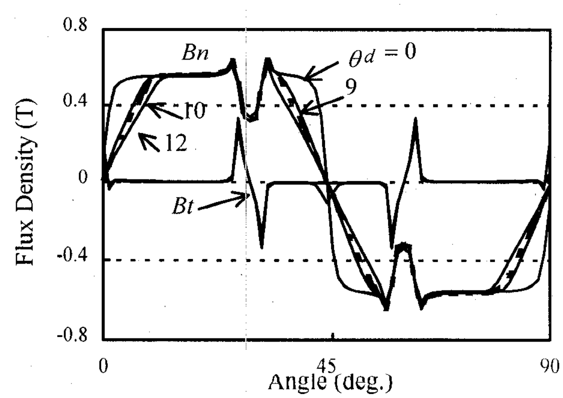

Fig. 3. Normal flux density B_n and tangential flux density B_t distribution in airgap for parameter θ_d .

Fig. 4 shows the 3-D finite element mesh of 90 degree symmetry model. Fig. 5 shows the magnetic flux density distribution in air gap for aligned detent position by using 3-D FEM. The comparison of Fig. 3 and Fig. 5 shows a reasonable agreement.

Fig. 6 shows the distribution of the flux density vector in *r*-*z* cross section by 3-D EMCN. The remarkable leakage flux in overhang section can be seen, which can not be considered by 2-D analysis.

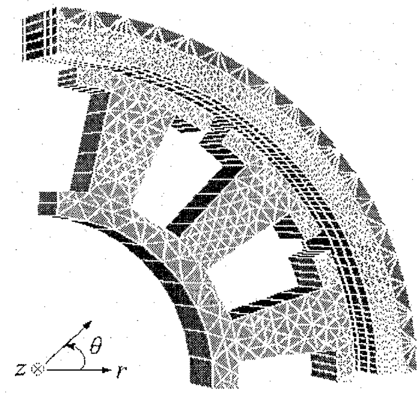

Fig. 4. 3-D FEM mesh of analysis model.

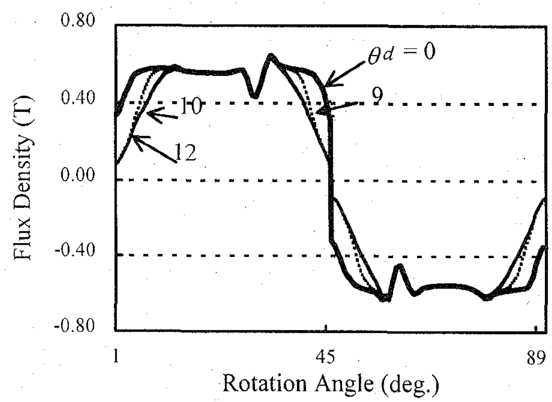

Fig.5. Flux density distribution in airgap for parameter θ_d by 3-DFEM.

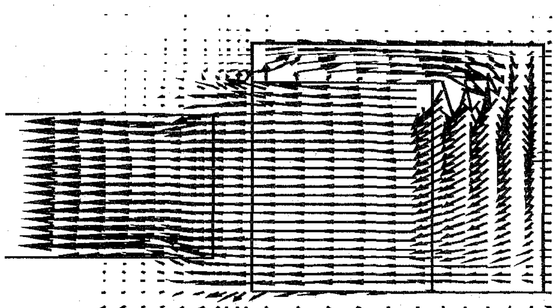

Fig.6. Distribution of the flux density vector in *r-z* cross section.

Fig. 7 shows the comparison of analysis result and experimental one of cogging torque for one period, 15 degrees which is governed by the permanent magnet and the tooth geometry only. The dead zone angle θ_d is 7.5 degree.

Fig. 8 shows comparison of frequency analysis of experimental data and simulation data using discrete Fourier transform. As will be seen, good agreement is achieved with excitation frequency which is integer multiple of 24.

Fig. 9 shows the variation of cogging torque according to variation of dead zone angle, θ_d. Cogging torque gradually decreases at about θ_d=10°, and then increases in reverse direction.

Fig. 10 shows the driving frequency components of the cogging torque which are integer multiple of the least common multiple of the number of poles and the number of teeth for each dead zone angle.

From the results in Fig. 9 and Fig. 10, the results of simulation is good agreement with calculated value, excitation frequency which is integer multiple of 24. The minimum of cogging torque is obtained by the model with dead zone angle, θ_d=10°.

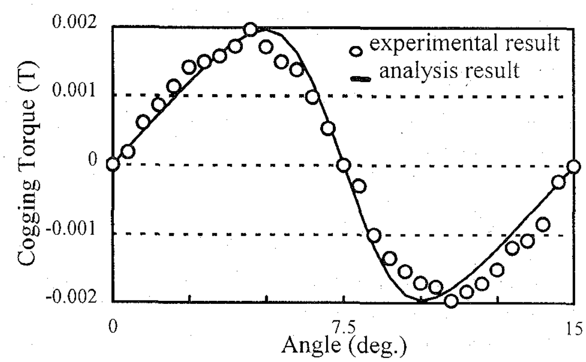

Fig. 7. Comparison of analysis result and experimental one for dead zone angle θ_d =7.5 degree.

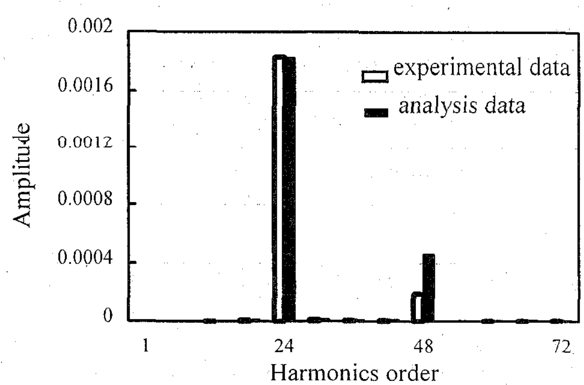

Fig.8. Comparison of frequency analysis of simulation result and experimental ones for dead zone angle θ_d =7.5 degree.

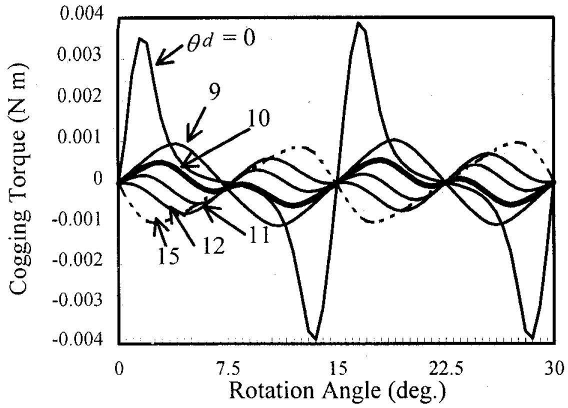

Fig. 9. Cogging torque vs. rotation angle for 6 models changing the dead zone angle θ_d.

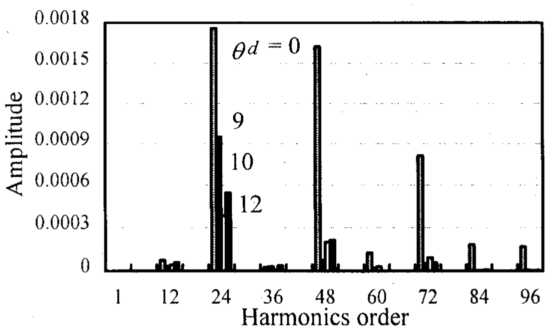

Fig. 10. Frequency analysis of cogging torque for 4 models changing the dead zone angle θ_d=0, 9, 10, 12 degrees respectively.

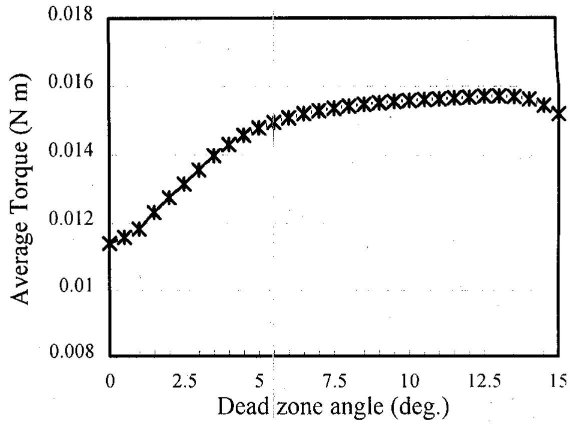

Fig. 11. Average torque according to variation of the dead zone angle θ_d.

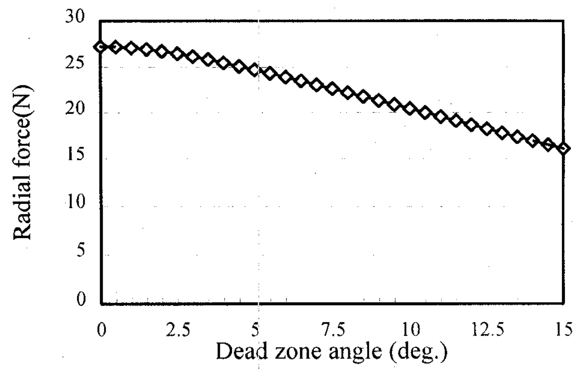

Fig. 12. Radial force according to variation of the dead zone angle θ_d.

Fig. 11 shows the effect of dead zone angle θ_d on average torque at starting position when BLDCM is driven by using 3 phase full wave excitation. Average torque becomes maximum value near θ_d=13°.

Fig. 12 presents the variation of radial force due to the change of dead zone angle from 0 degree to 15 degree increasing by 0.5 degrees. The radial force is decreased by increasing the dead zone angle. From Fig. 11 and Fig. 12, the best improvement of average torque is obtained near θ_d = 13°.

From the results, cogging and average torque is improved substantially according to the dead zone angle of trapezoidal magnetization distribution.

IV. Conclusion

The effect of variation of magnetization distribution in rotor magnet on the prediction of cogging torque in BLDCM has been discussed. The dead zone angle which minimizes the cogging torque giving the bad influence on the torque ripple is obtained. For the 3-D analysis considering the overhang 3-D EMCN is used and the analysis results are compared with the ones of experiment and 3-D FEM respectively.

The magnetization distribution is assumed to have trapezoidal shape. Though its shape has different form, the distribution is periodic so it could be represented by using Fourier series. 3-D EMCN is useful as the analysis tool for the permanent magnet motor such as linear synchronous motor, stepping motor, etc.

References

[1] T. Li and G. Slemon, "Reluctance of cogging torque in permanent magnet motors," *IEEE Trans. on Magn.* vol. 24, pp. 2901-2903, 1988.

[2] Takeo Ishikawa and Gordon R. Slemon, "A method of reducing ripple torque in permanent magnet motors without skewing," *IEEE Trans. on Magn.* vol. 29, no. 2, pp. 2028-2031, 1993.

[3] Z. Q. Zhu and D. Howe, "Analytical prediction of the cogging torque in radial-field permanent magnet brushless motor," *IEEE Trans. Magn.* vol. 28, pp. 1371-1374, 1992.

[4] T. Nakata, N. Takahashi and K. Uehara "Analysis of magnetic characteristics of a brushless dc motor taking into account the distribution of magnetization," *IEEE Trans on Magn*, vol. 22, no. 5, pp1084-1086, 1986.

[5] Y. Kawase, T. Yamaguchi, "Analysis Cogging Torque of Permanent Magnet Motor by 3-D Finite Element Method," *IEEE Trans on Magn.* vol.31, no. 3, pp.2111-2113, 1995.

[6] J. Hur, S. B. Yoon, D. Y. Hwang and D. S. Hyun, "Analysis of PMLSM using 3 dimensional equivalent magnetic circuit network method," *IEEE Trans. on Magnetics*, vol. 33, no. 5, pp. 4143-4145 1997.